HIPPOCAMPUS 22:2260–2275 (2012)

CGG Trinucleotide Repeat Length Modulates Neural Plasticity and Spatiotemporal Processing in a Mouse Model of the Fragile X Premutation

Michael R. Hunsaker,[1*] Kyoungmi Kim,[2] Rob Willemsen,[3,4] and Robert F. Berman[1,4]

ABSTRACT: The fragile X premutation is a CGG repeat expansion on the *FMR1* gene between 55 and 200 repeats in length. It has been proposed that impaired spatiotemporal function underlies cognitive deficits in genetic disorders, including the fragile X premutation. This study characterized the role of the premutation for cognitive function by demonstrating CGG KI mice with 70–198 CGG repeats show deficits across tasks requiring spatial and temporal pattern separation. To elucidate mechanisms whereby CGG repeats affect spatiotemporal processing, hippocampal slices were evaluated for LTP, LTD, and mGluR1/5 LTD. Increasing CGG repeat length modulated the induction of LTP, LTD, and mGluR1/5 LTD, as well as behavioral tasks emphasizing spatiotemporal processing. Despite the deficits in the induction of all forms of plasticity, there were no differences in expression of plasticity once evoked. These data provide evidence for a neurocognitive endophenotype in the CGG KI mouse model of the premutation in which CGG repeat length negatively modulates plasticity and spatiotemporal attention. © **2012 Wiley Periodicals, Inc.**

KEY WORDS: fragile X permutation; CGG KI mouse; long-term potentiation; long-term depression; pattern separation; temporal order; spatial processing; spatiotemporal hypergranularity; pattern separation; endophenotype

INTRODUCTION

The fragile X premutation is a CGG trinucleotide repeat expansion between 55 and 200 repeats in length on the fragile X mental retardation 1 (*FMR1*) gene. The premutation results in a 2–8 fold increase in *FMR1* mRNA levels in leukocytes and reduced *FMR1* protein (FMRP) levels (Tassone et al., 2000a,b, 2008). In fragile X syndrome (FXS) there are >200 CGG repeats, resulting in virtually undetectable *FMR1* mRNA and FMRP levels due to transcriptional silencing (Tassone et al., 2008; Hunsaker et al., 2011a).

[1] **Department of Neurological Surgery, School of Medicine, University of California, Davis; Davis, California;** [2] **Division of Biostatistics, Department of Public Health Sciences, School of Medicine, University of California, Davis; Davis, California;** [3] **CBG-Department of Clinical Genetics, Erasmus MC, Rotterdam, The Netherlands;** [4] **NeuroTherapeutic Research Institute, University of California, Davis, Davis, California**

Grant sponsor: National Institute of Health (NIH); Grant number: NINDS RL1 NS062411; Grant sponsor: Roadmap Initiative grant, NIDCR; Grant number: UL1 DE019583; Grant sponsor: NeuroTherapeutics Research Institute (NTRI), NCRR; Grant number: UL1 RR024146

*Correspondence to: Michael R. Hunsaker, Department of Neurological Surgery, 1544 Newton Court, Davis, CA 95616, USA.
E-mail: ryanhunsaker@me.com

Accepted for publication 10 May 2012
DOI 10.1002/hipo.22043
Published online 18 June 2012 in Wiley Online Library (wileyonlinelibrary.com).

Until recently, premutation carriers have been largely presumed to be cognitively unaffected by the mutation (Hunter et al., 2009, 2010). However, potential neurocognitive effects of the premutation have been reported (Koldewyn et al., 2008; Cornish et al., 2009; Keri and Benedek, 2009, 2010; Goodrich-Hunsaker et al., 2011a,b,c; Hessl et al., 2011). These studies suggest cognitive function in premutation carriers are modulated by the dosage of the *FMR1* mutation (i.e., increasing CGG repeat length), such that performance deteriorates as the CGG repeat length increases.

Simon (2008, 2011) proposed that neurogenetic disorders including fragile X-associated disorders, Turner syndrome, Williams syndrome, and 22q11.2 deletion syndrome have overlapping cognitive impairments involving spatiotemporal attention that result from reductions in the resolution, or clarity, of mental representations, referred to as a spatiotemporal hypergranularity. As such, discriminating spatial distances or temporal separations among stimuli becomes increasingly difficult as the spatial or temporal differences become smaller due to increasing interference (cf., Hunsaker, 2012). Thus, many individuals with neurogenetic disorders have relatively coarse mental representations, so identification of one spatial location or time point from another requires a larger between-item difference before the two can be perceived as distinct (cf., Hanson and Madison, 2011).

It has been demonstrated that the hippocampus is critical for processing spatial and temporal relationships between stimuli in such a way that incoming sensory information is orthogonalized to minimize interference across both time and space via a process called pattern separation (Kesner et al., 2004; Rolls and Kesner, 2006; Kesner, 2007). It is likely that impaired hippocampus-dependent spatial and temporal pattern separation contributes to the spatiotemporal hypergranularity observed in genetic disorders, including the fragile X premutation (Hanson and Madison, 2011).

To characterize the molecular effects disrupted by the fragile X premutation, Willemsen et al. (2003) generated a CGG KI mouse model of the premutation via homologous recombination in which the mouse 5′ untranslated region containing 8-12 CGG repeats on the *Fmr1* gene was replaced with a 5′

untranslated region containing 98 CGG repeats of human origin. Importantly, the CGG KI mouse recapitulates the molecular phenotypes observed in the human premutation: CGG KI mice show two to five times elevated levels of *Fmr1* mRNA and 20–30% reductions in Fmrp levels that scale with CGG repeat length (Brouwer et al., 2008). Another model of the premutation was generated by Entezam et al. (2007) by serial ligation of CGG-CCG repeats in the 5′ untranslated region in the mouse *Fmr1* gene. This mouse shows similar elevations in *Fmr1* mRNA levels, but profound reductions in Fmrp expression that are not present in the human fragile X premutation. Both mouse models have been tested using behavioral screens evaluating spatial memory, motor function, anxiety, and social behavior (van Dam et al., 2005; Qin et al., 2011); but the results of these tasks failed to recapitulate altered neurocognition as reported carriers of the fragile X premutation. As such, the present experiment used the CGG KI mice as subjects to be more directly comparable with the cognitive research into carriers of the fragile X premutation (cf., Goodrich-Hunsaker et al., 2001a,b,c).

This study was designed to firmly establish the effects of increasing CGG repeat length for spatiotemporal attention by testing CGG KI mice with 70–198 CGG repeats in length on behavioral tasks requiring spatial and temporal pattern separation. To elucidate mechanisms whereby increasing CGG repeats may affect spatiotemporal processing, mice were evaluated for induction and expression of NMDA receptor-dependent long-term potentiation (LTP) and long-term depression (LTD) and mGluR1/5 dependent LTD at the Schaffer collateral synapse in acute hippocampal slices. The data provide the first demonstration that CGG KI mice have a spatiotemporal hypergranularity as well as reduced hippocampal plasticity induction, both of which are modulated by the dosage of increasing CGG trinucleotide repeat lengths. Together these data provide evidence for a behavioral endophenotype, and provides a candidate mechanism whereby increasing CGG repeat lengths may negatively impact cognitive function.

MATERIALS AND METHODS

Animals

Forty-eight male CGG KI mice and 24 wildtype (WT) littermate mice were used as subjects for this task. CGG KI mice were mice with 70–116 CGG repeats (Low CGG n = 24) and mice with 132–198 CGG repeats (High CGG n = 24). These groups emerged during breeding and are grouped in this manner because of the 16 CGG repeat gap between the groups, not to model any known difference between these repeat length groups in human premutation carriers. CGG KI mice were on a congenic C57BL/6J background. All mice were 9 months of age (±0.32 SEM) at the beginning of experimentation to model the effects of the premutation during mid to late adulthood in human premutation carriers. Mice were housed in same sex, mixed genotype groups with one to four mice per cage on a 12 h light–dark cycle. Mice were maintained at 90-95% of their free feeding weight and had ad libitum access to water during experimentation. All experiments conformed to UC Davis IACUC approved protocols and all effort was taken to reduce stress in all mice during experimentation.

Genotyping

As somatic instability of CGG repeats on the *Fmr1* gene among tissues in the CGG KI mouse has been shown to be negligible (typically under 10 CGG repeats across tissues; Willemsen et al., 2003), genotyping to verify CGG repeat length was carried out upon tail snips. Following a method kindly provided by Rob Willemsen (Brouwer et al., 2008) and modified in collaboration with the laboratories of F Tassone and P Hagerman (Salute et al., 2005, F Tassone personal communication), CGG repeat lengths were measured using the FastStart Taq DNA Polymerase, dNTP Pack (Roche Diagnostics; Manheim, Germany) DNA was extracted from mouse tails by incubating with 10 mg/mL Proteinase K (Fermentas, Glen Burnie, MD) in 300-μL lysis buffer containing 50 mM Tris-HCl, pH 7.5, 10 mM EDTA, 150 mM NaCl, 1% SDS overnight at 55°C. One hundred microliters (100 μL) saturated NaCl was then added, mixed, and centrifuged. The supernatant was gently mixed with two volumes of 100% ethanol, and the DNA was pelleted by centrifugation. The DNA was washed and centrifuged in 500 μL 70% ethanol. The DNA was then dissolved in 100 μL reverse osmosis distiller water. CGG repeat lengths were determined by PCR using solutions from the FastStart Taq DNA Polymerase, dNTP Pack (Roche Diagnostics). Briefly, approximately 500–700 ng of DNA was added to 20 μL of PCR mixture containing 0.5 μM/L of each primer, 250 μM/L of each dNTP (Roche Diagnostics), 2.5 M Betaine (Sigma-Aldrich), 1X Buffer 2 and 0.05 U of FastStart Taq DNA Polymerase (Roche Diagnostics). The primers flank the CGG repeat region of *Fmr1* gene, the forward primer was 5′-CGG GCA GTG AAG CAA ACG-3′and the reverse primer was 5′-CCA GCT CCT CCA TCT TCT CG-3 The CGG repeats were amplified using a 3-step PCR with 10 min denaturation at 98°C, followed by 35 cycles of 35 s denaturation at 98°C, annealing for 35 s at 55°C, and at the end each cycle elongation for 2 min at 72°C. The last step of the PCR consisted in a 10 min elongation at 72°C. The sizes of CGG DNA amplicons were determined by running 20 μL of PCR reaction per sample and a molecular weight marker (O'GeneRuler 50bp DNA ladder; Fermentas) for 2 h at 150 V on a 2.5% agarose gel with 0.03 μL/mL ethidium bromide. The number of CGG repeats was calculated from pictures acquired with a GelDoc-It Imaging system (UVP, LLC Upland, CA) and using VisionWorks LS software (UVP, LLC). This method can detect up to 358 CGG repeats from animals in the present mouse colony). Genotyping was performed twice on each mouse, once using tail snips taken at weaning and again on tail snips and/or brain tissue collected at sacrifice. In all cases the genotypes matched.

Experimental Design

The order in which the four behavioral tasks were presented to each mouse was randomized in the WT group, and 7 days separated each task; furthermore, the order during each testing session during which a given mouse was tested was randomized. Once behavior was finished, all mice were prepared for physiology. For physiology, the order of experiments was randomized across slices within each mouse. From each mouse, three sequential hippocampal slices were evaluated from the dorsal-intermediate hippocampus (sections taken between 1 and 3.5 mm caudal to the septal pole of the hippocampus). The order in which slices were used, as well as which form of plasticity was evaluated on which slice were randomized and order was included as a covariate in all statistical analyses. For both behavior and physiology, each WT mouse was paired with an individual CGG KI mouse with 70–116 CGG repeats as well as an individual CGG KI mouse with 132–198 CGG repeats as an explicit control for potential effects of experimental order in task performance across CGG repeat groups. Experimental order was included as a covariate in all statistical analyses.

Behavioral testing took place between 9 and 10 months of age for all mice and physiology took place between 10 and 13 months of age for all mice. Importantly, all mice used for behavior were also used for physiological studies. To control for potential effects of mouse age during physiology, mouse age was used as a covariate in all physiological data analyses.

Coordinate and Categorical Spatial Processing Tasks

Behavioral apparatus

For the coordinate and categorical spatial processing tasks (Hunsaker et al., 2009; called "metric" and "topological" in that study) a circular table measuring 1 m in diameter was covered with a white, plastic sheet (i.e., shower curtain). Four objects measuring between 2.5 and 5 cm in diameter at the base and between 5 and 15 cm tall were used as stimuli. The table was enclosed by four white curtains 1 m away from the table edge with visually complex distal cues placed at the same level as the table surface affixed to the curtains.

Between the habituation and test sessions, the mice were placed in an opaque holding cup. The circular table was wiped down with 70% ethanol after each mouse to reduce and mask olfactory cues. All trials were digitally recorded by a camera located above the tabletop that was connected to a computer running ANY-maze behavioral tracking software (v4.3; Stoelting; Wood Dale, IL).

Behavioral Methods

Coordinate spatial processing task

Each mouse was placed on the edge of the table facing two objects placed 45 cm apart. The mouse was allowed 15 min to freely explore the tabletop, objects, and distal environment. Exploration of the objects decreased over the 15 min period as animals habituated. After the 15 min habituation session, the mouse was removed to the small holding cup for 5 min. During this intersession interval, the objects were shifted 15 cm closer to each other so that the objects were now spaced 30 cm apart. After the objects were shifted closer together, the mouse was placed on the table and given 5 min to explore the objects during the test session.

Categorical spatial processing task

For the categorical spatial processing task, two novel objects, different from those used for the coordinate task, were used as stimuli. Mice were placed on the table and allowed to habituate to the objects exactly as in the coordinate task, and then removed from the table for 5 min. During the 5 min between the habituation and test sessions, the objects were transposed, such that the left object was now on the right side and vice versa, but the spatial locations occupied by objects were held constant.

Dependent Measures

For both the coordinate and categorical tasks, the time spent exploring each object was recorded as the dependent variable. Exploration was defined as the mouse actively sniffing or touching the object with its nose, vibrissa, mouth, or forepaws. An animal simply located near or standing on top of the objects without actively interacting with them was not scored as exploration. Object exploration data were summarized in 5 min epochs during the 15 min habituation period to facilitate comparison with the 5 min test session, as previously described (Hunsaker et al., 2009). Mice habituated to the objects during the 15 min habituation phase, and show relatively low levels of exploration during the last 5 min compared to the first 5 min. However, during the 5 min test session when mice are returned to the table, mice that remember the object distance (coordinate or metric) or object position (categorical or topological) show increased exploration of the objects. Locomotor activity was collected by the ANY-maze system.

Statistical Methods

Locomotor activity was analyzed using a 3 (binned CGG repeat group) $\times$ 4 (session; three 5 min bins during habituation, test session) repeated measures analysis of covariance (ANCOVA). Experiment order was included as a covariate in the analysis. Total object exploration time during the 15 min habituation session was calculated for the first, second, and last 5 min epochs to facilitate comparison between the last 5 min of the habituation session and the 5 min test session. A 3 (CGG repeat group) x 3 (session) repeated measures ANCOVA was performed on these exploration data for both coordinate and categorical spatial processing tasks, with experiment order as a covariate in the analysis.

To facilitate the comparison between the test session and the last 5 min of the habituation session, an exploration ratio was

calculated as: [(exploration time during the 5 min test session)/(exploration time during the 5 min test session + exploration during the last 5 min of the habituation session)]. This constrained all values between 0 and 1. With this ratio, increased exploration during the 5 min test session compared with the last 5 min of the habituation session is reflected as a ratio > 0.5, and decreased exploration (or continued habituation) is reflected as a ratio < 0.5. Prior to comparing CGG KI mice and WT mice for the ratio scores, it was verified that the ratio score for the WT mice was $\neq .5$ via a one-tailed *t*-test against the null hypothesis of a ratio score $= 0.5$, suggesting heightened exploration of the objects during the test session compared to the final 5 min of the habituation session.

To compare ratios between CGG KI mice and WT mice, one way ANCOVA with CGG repeat group as the grouping variable were performed for both coordinate and categorical tasks, with experiment order as a covariate. To more directly elucidate a role for CGG repeat length modulation of any effects within the CGG KI mice, two-tailed Pearson's correlation coefficients were calculated to assess the relationship of the ratio values with CGG repeat length in only the CGG KI mice.

Temporal Ordering for Visual Objects Task

Behavioral apparatus

To evaluate temporal ordering in CGG KI mice as a function of CGG trinucleotide repeat length, mice were tested on a temporal ordering for visual objects task (Hunsaker et al., 2010). The task was run in a transparent Plexiglas box 26 cm long × 20 cm wide × 16 cm tall. Eight objects in triplicate were used as stimuli for this study. These objects ranged in size from 6 cm diameter × 6 cm tall to 4 cm × 2 cm. All objects and the apparatus were wiped down with 70% ethanol between sessions in order to reduce odor cues.

Behavioral Methods

Temporal ordering for visual objects task

During session 1, two identical copies of a first object (object 1) were placed at the ends of the box 2.5 cm from the end walls and centered between the long walls. The mouse was placed in the center of the box facing away from both objects. The mouse was given 5 min to freely explore the objects. After 5 min, the mouse was removed to a small holding cup for 5 min. During this time, the first objects were replaced with two duplicates of a second object (Object 2). For Session 2, the mouse was again placed in the apparatus and allowed to explore. After 5 min, the mouse was removed to the holding cup for 5 min and the objects were replaced with two duplicates of a third object (Object 3). For Session 3, the mouse was given 5 min to explore. After 5 min, the mouse was removed into a small cup for 5 min and an unused copy of the first and an unused copy of the third object were placed into the box. The mouse was again placed into the box and allowed to explore the two objects (i.e., Objects 1 and 3) during a 5 min test session. All trials were recorded by a camera located directly above the tabletop that was connected to a PC laptop computer running ANY-maze behavioral tracking software.

Mice typically show increased exploration of the first object compared to the third object, and this was used as an index of memory of the temporal order of the object presentation. A lack of preferential exploration of one object over the other indicates temporal ordering impairments.

Visual object novelty detection task

In addition to reflecting impaired temporal ordering, increased exploration of the first object over the third could also be interpreted as being due to difficulty in remembering the first object prior to the test session. To minimize and control for such general memory deficits, a novelty detection of visual objects task was performed. Briefly, on a different day mice received three sessions during which they were allowed to explore three novel sets of objects (Objects 4, 5, 6) similarly to the temporal ordering tasks. During the test session, the first object and a novel fourth object (Object 7) were presented and the mice were allowed 5 min to explore. Preferential exploration of the novel Object 7 over Object 4 would indicate that the mouse remembered having previously explored Object 4, whereas equal levels of exploration of the two objects would indicate that forgetting had occurred.

Dependent measures

For the temporal ordering task, object exploration was defined as active physical contact with the object with the forepaws, whiskers, or nose. With this definition, a mouse standing near an object without interacting with it would not be counted as exploration. To control for differences in exploration levels between mice, exploration during the temporal ordering test sessions was converted into a ratio score to constrain the values between −1 and 1. The ratio calculated as follows: (exploration of Object 1 − exploration of Object 3)/(exploration of Object 1 + exploration of Object 3). Exploration during the novelty detection test sessions was similarly converted into a ratio score, using exploration of Objects 4 and 7 in the calculation: (exploration of novel Object 7 − exploration of Object 4)/(exploration of Object 4 + exploration of novel Object 7).

A ratio value near 1 means that the mouse showed more exploration of the first item presented in the temporal ordering task. A score near −1 suggests the mouse preferentially explored the last object presented. A score near 0 reflects equal exploration of objects indicating a failure to detect the temporal order of visual object presentation.

In the novel object test a score approaching either 1 (i.e., preference for the novel Object 7) or −1 (preference for Object 1) would indicate intact memory of Object 4, while a score near 0 would suggest that forgetting had occurred. As a measure of general activity levels, locomotor activity was determined by recording the number of times the mouse crossed the midline of the box with all four paws during each session.

Statistical Methods

Locomotor activity was analyzed using a 3 (binned CGG repeat group) × 4 (session) repeated measures ANCOVA. Experiment order was included as a covariate in the analysis. Any differences in locomotor activity were more fully characterized using Tukey's HSD post hoc pairwise comparisons test when the overall group comparison was significant. Object exploration data from each session were analyzed with 3 (CGG repeat group) × 4 (session) repeated measures ANCOVA with experiment order as a covariate to verify that mice explored all the objects similarly during the study sessions to verify that unequal exploration would not confound measures of temporal ordering. Furthermore, side preferences during object Sessions 1–3 were tested with individual paired *t*-tests against the null hypothesis of 50% exploration for the object on each side. Prior to comparing CGG KI mice and WT mice for the ratio scores, it was verified that the ratio score for the WT mice was =.0 via a one-tailed *t*-test against the null hypothesis of a ratio score = 0 to verify preferential exploration of the first object during the temporal order test and novel object during the novelty test.

Exploration data that were converted to ratio values were analyzed by one-way ANCOVA with experiment order as a covariate. To more fully characterize any differences among groups, Turkey's HSD post hoc pairwise comparisons test was performed when the overall group comparison was significant. To verify that locomotor behavior and object exploration during earlier sessions did not contribute to temporal ordering and/or novelty detection measures recorded during the test sessions, ANCOVA were performed with both locomotor behavior and object exploration during Session 1, both locomotor behavior and object exploration during Session 3, as well as locomotor behavior during the test session as covariates, as well as experiment order. To elucidate a role for CGG repeat length modulation of any effects within the CGG KI mice, Pearson's correlation coefficients were calculated to assess the relationship of the ratio values with CGG repeat length in only the CGG KI mice.

Neurophysiology

Slice preparation

Mice were anesthetized with isoflurane, decapitated, and the brains were rapidly transferred to cold, oxygenated artificial CSF (aCSF) containing (in mM) 124 NaCl, 3 KCl, 1.25 NaH_2PO_4, 2 $MgSO_4$, 26 $NaCO_3$, 2 $CaCl_2$, and 10 dextrose. Brains were then blocked in the coronal plane to contain the hippocampus; a Vibratome (Vibratome Company; St. Louis, MO) was used to cut 400 μm-thick slices transverse to the longitudinal axis of the hippocampus into a bath of oxygenated aCSF at 1°C. Individual slices, from the dorsal/intermediate third of the hippocampus, were placed in a holding chamber at 30°C with oxygenated aCSF and allowed to equilibrate for at least 60 min before transfer to a slice interface recording chamber (Fine Science Tools; Foster City, CA) for electrophysiological experiments. Slices rested on a nylon mesh over a well perfused with warmed (32–35°C), oxygenated aCSF (2 mL/min perfusion rate); the slice surface was exposed to a warmed, humidified 95% O_2 /5% CO_2 environment. Slices were exposed to this environment for 30 min prior to the placement of any electrodes, and an additional 10 min after electrode placement prior to delivery of any stimuli.

Neurophysiological Methods

Field evoked post synaptic potentials (fEPSPs) were recorded with extracellular electrodes made from borosilicate glass pulled on a horizontal puller (Sutter Instruments; Novato, CA) and filled with 0.1 M NaCl (∼5 MΩ resistance) and placed in the middle of the stratum radiatum in distal CA1. Synaptic responses were evoked by a 200-μs current pulse to Schaffer collateral axons in proximal CA1 near the CA2/CA3 border with a concentric bipolar tungsten stimulating electrode connected to a stimulus isolation unit (World Precision Instruments; Sarasota, FL). Stable baseline responses were collected every 30 s after adjusting stimulus intensity (10–30 μA) to achieve 50% of the maximal fEPSP slope in the absence of population spikes. Only slices in which fEPSPs in which maximal amplitudes >1.5 mV could be maintained for 15 min were used (in total, 15% of slices were discarded for failure to meet this threshold).

Plasticity Induction Methods

NMDA receptor-dependent long-term potentiation (LTP) of fEPSPs was induced using a conditioning stimulus consisting of four trains of 50 pulses at 100 Hz, 30 s apart (high-frequency stimulation; HFS). NMDA receptor-dependent long-term depression (LTD) of fEPSPs was induced using conditioning stimulus of 900 pulses delivered at 1 Hz delivered over 15 min (low-frequency stimulation; LFS). Metabotropic GluR1/5 (mGluR1/5) receptor-dependent LTD was induced by applying 3,5-dihydroxyphenylglycine (DHPG) into the perfusing medium (50 μM final concentration perfused across the tissue at 2 mL/min) and continuing with baseline stimulation for 15 min followed by immediate washout.

R,S-DHPG was purchased from Tocris (St. Louis, MO). All other chemicals were purchased from Sigma. DHPG was prepared as a 100 times stock in H_2O, aliquoted and stored at −20°C. Fresh stocks were made once a week and diluted in aCSF to achieve their final concentrations for perfusion application.

Histology

After performing neurophysiological analyses, the hippocampal slices were placed in 4% buffered paraformaldehyde for 24 h at room temperature on a shaker table before being cryoprotected in 10% and 30% sucrose and flash frozen. In total, 30-μm sections from a random subset of hippocampal slices that were recorded from were stained for hematoxylin and eosin and evaluated for viability and structural abnormalities that

may contribute to any differences among mice for physiological measures.

Dependent Measures

All electrophysiological data were recorded using an Axoclamp 2A amplifier (Axon Instruments; Foster City, CA), high pass filtered at 3 Hz, low-pass filtered at 10kHz, digitized (20 kHz) using an Axon Digidata 1200 digital acquisition system (Axon Instruments), and stored on a personal computer system. Data were quantified with Axoscope software (Clampfit 10.0; Axon Instruments) to evaluate the slope of the fEPSP from 10 to 90% of the rising phase of the potential. All data were plotted using Datagraph 3 (Visual Data Tools; Chapel Hill, NC), and are reported as % (±SEM) of the baseline (preconditioning) values. For analysis, data collected over 60 min post induction of plasticity were collected and the mean of the two responses evoked during each 1 min bin were used as the unit of analysis. Furthermore, mean fEPSP slope from each mouse averaged over 10–20 min post conditioning were used for correlation analyses, as was mean fEPSP slope averaged over 40–50 min post conditioning.

Statistical Methods

To determine differences among groups for plasticity, a 3 (binned CGG repeat group) × 60 (min) repeated measures ANCOVA was performed for each of NMDA receptor-dependent LTP and LTD, as well as mGluR1/5 dependent LTD. Experiment order and mouse age were included as covariates.

To further evaluate any differences in physiological measurements among CGG repeat groups, the mean level of LTP or LTD (fEPSP slope relative to baseline) between 10 and 20 min post conditioning stimulus or DHPG application was evaluated by comparing CGG groups by ANCOVA with experiment order and mouse age as covariates, as was mean fEPSP slope 40–50 min post conditioning.

To elucidate a specific role for CGG repeat length modulation of any effects within the CGG KI mice, Pearson's correlation analyses were performed to determine the relationship of the mean fEPSP slope between min 10–20 and min 40–50 post induction with CGG repeat length in only the CGG KI mice.

Omnibus Statistical Methods

Hypothesis testing

Prior to statistical analyses, the data were tested for normalcy (Shapiro–Wilk test) and homoscedacity (Browne–Forsythe test). To account for any potential effects of order or multiple comparisons arising from performing ANCOVA and correlation analyses on four separate behavioral datasets as well as three plasticity datasets all collected from the same animals, a 3 (group) × 4 (task) multivariate analysis of covariance (MANCOVA) was performed with experiment order and mouse age as covariates. Main effects of the MANCOVA were characterized by individual ANCOVA. All results were considered significant at $\alpha \leq 0.05$ and $1-\beta \geq 0.8$, and analyses were performed to determine observed power and effect size of all main effects. Statistical analyses were performed in R 2.13.1 language and environment (R Development Core Team, 2011) and statistical power was calculated using both R and the statistical program G*Power 3 (Faul et al., 2007, 2009). All reported p values were adjusted for False Discovery Rate (FDR; Benjamini et al., 2001) using a custom script written in R 2.13.1.

Unsupervised cluster analysis

Initial characterization and clustering of the data were performed using unsupervised hierarchal clustering in R 2.13.1. Hierarchal cluster analysis was performed to organize subjects into clusters such that subjects within a cluster are more "similar" to each other than they are to subjects in the other clusters based on a measure of their similarity/dissimilarity in behavioral and neurophysiological measurements and to show how the different clusters are related to each other. The process starts with each subject in a separate cluster and then combines the clusters sequentially, reducing the number of clusters at each step. At each stage, distances between clusters were computed by Ward's linkage algorithm (i.e., to minimize the increase in the mean error sum of squares (Ward, 1963)). The dendrograms were examined for separation or clusters relating to the three groups of CGG repeat length, WT, Low CGG repeat, and High CGG repeat groups.

Support vector machines classification and validation

Further, support vector machines (SVM), a supervised machine learning technique, were performed to determine whether patterns in the behavioral and neurophysiological data can be interpreted as indications of the expansion of CGG repeat length. SVM are linear classifiers that seek to find the optimal (i.e., provides maximum margin) hyperplane separating groups using patterns of all measurements. The margin is defined as the distance between the hyperplane and the samples of the two classes (CGG KI vs. WT) that are closest to the hyperplane among those being correctly classified. To assess the performance of the SVM classifier, iterative *k*-fold cross validation (10-fold, 5-fold, 3-fold, and leave-one-out cross validation) methods were used to estimate the accuracy of the classifier that predicts the group classification of a test sample. For *k*-fold cross validation (CV), the data set is randomly split into a training set for model construction and a test set for assessing predictive performance- this procedure is repeated, leaving out each test set at a time until all samples in the test set have been classified and then averaging the prediction error rates over all the possible test sets. For subsequent analyses the WT mice were removed from the dataset and the analyses were repeated to verify that CGG KI mice could be correctly classified by CGG repeat length (i.e., Low CGG repeat vs. High CGG repeat).

TABLE 1.

Summary of Experimental Results

Experiment	Wildtype	Low CGG (CGG 70–116)	High CGG (CGG 132–198)	$P_{(adj)}$ value	Correlation with CGG repeat
Behavior					
Coordinate	0.65 ± 0.01	0.56 ± 0.01	0.48 ± 0.02	$P_{(adj)} = 3.09e^{-13}$	$\rho = -0.71$; $R^2_{(adj)} = 0.51$
Categorical	0.64 ± 0.01	0.57 ± 0.01	0.50 ± 0.02	$P_{(adj)} = 4.9e^{-9}$	$\rho = -0.57$; $R^2_{(adj)} = 0.34$
Temporal	0.65 ± 0.03	0.56 ± 0.01	0.11 ± 0.01	$P_{(adj)} = 1.2e^{-14}$	$\rho = -0.77$; $R^2_{(adj)} = 0.60$
Novelty	0.38 ± 0.03	0.38 ± 0.03	0.36 ± 0.02	$P_{(adj)} = 0.96$	$\rho = -0.09$; $R^2_{(adj)} = 0.02$
Physiology					
NMDAR LTP					
min 10–20	273.24 ± 3.7%	248.22 ± 6.4%	240.30 ± 4.5%	$P_{(adj)} = 2.4e^{-15}$	$\rho = -0.59$; $R^2_{(adj)} = 0.62$
min 40–50	189.31 ± 18.9%	181.01 ± 6.8%	169.79 ± 14.3%	$P_{(adj)} = 0.15$	$\rho = -0.10$; $R^2_{(adj)} = 0.09$
NMDAR LTD					
min 10–20	57.35 ± 3.5%	76.23 ± 3.7%	84.92 ± 4.2%	$P_{(adj)} = 2.4e^{-15}$	$\rho = 0.74$; $R^2_{(adj)} = 0.46$
min 40–50	73.75 ± 6.5%	78.01 ± 5.6%	82.00 ± 6.7%	$P_{(adj)} = 0.45$	$\rho = 0.02$; $R^2_{(adj)} = 0.01$
mGluR1/5 LTD					
min 10–20	48.65 ± 4.0%	60.90 ± 3.9%	74.28 ± 3.2%	$P_{(adj)} = 2.4e^{-15}$	$\rho = 0.64$; $R^2_{(adj)} = 0.59$
min 40–50	85.75 ± 6.6%	92.20 ± 8.1%	85.01 ± 10.24	$P_{(adj)} = 0.54$	$\rho = 0.05$; $R^2_{(adj)} = 0.03$

Mean (±standard error of the mean) ratio values for behavioral experiments and mean (±SEM) % change in fEPSP slope relative to baseline for minutes 10–20 and minutes 40–50 post conditioning for Wildtype and CGG KI mice. Correlations between experimental performance and CGG repeal length within the CGG KI mice are also presented. All P values were adjusted for false discovery rate, as were all R^2 values.

RESULTS

Multivariate Analysis of Covariance

Prior to performance of any statistical analyses, it was determined that all individual data sets met the assumptions for the usage of parametric statistics; that is the data were normally distributed and homoscedastic. An omnibus MANCOVA demonstrated that there were no significant effects of experiment order for performance on behavioral tasks or measure of neural plasticity ($P_{(adj)} = 0.26$), nor were there effects for mouse age ($P_{(adj)} = 0.43$). There was a significant effect of CGG repeat group for experimental performance ($F(14,116) = 47.57$, $P_{(adj)} < 2e^{-16}$, 1-ß = 0.98). The main effect of group was characterized by individually evaluating each experiment and we are reporting p values corrected for multiple comparisons across all analyses using the false discovery rate procedure (Benjamini et al., 2001). Furthermore, there were no differences in structural integrity or cellular viability among hippocampal slices across groups that would have contributed to group differences in physiological measures. Table 1 provides a summary of statistical analyses.

Coordinate Spatial Processing

For the coordinate task, there was a significant main effect of CGG repeat group ($F(2,65) = 51.56$, $P_{(adj)} = 3.9e^{-13}$, 1-ß = 0.98), and no effect of task order among groups for this task ($F(4,65) = 1.73$, $P_{(adj)} = 0.71$). Furthermore, there were no significant differences among groups for either locomotor behavior or object exploration during the 15 min habituation session (all $P_{(adj)} > 0.20$). Tukey's HSD post hoc pairwise comparisons demonstrated that the High CGG repeat group performed significantly worse than the Low CGG repeat group and WT group (both $P_{(adj)} < 0.001$), and the Low CGG group performed worse than the WT group ($P_{(adj)} < 0.01$).

To characterize any possible relationship between CGG repeat length and coordinate spatial processing in CGG animals with expanded CGG trinucleotide repeats, a correlation coefficient was calculated. A negative association was observed between the CGG trinucleotide repeat length and the ratio value during performance of the coordinate task (Fig. 1A; corr $\rho = -0.71$; $P_{(adj)} = 1.7e^{-15}$, $R^2_{(adj)} = 0.51$), suggesting that the coordinate spatial processing is inversely related with the CGG repeat length.

Categorical Spatial Processing

For the categorical task, there was a significant main effect of CGG repeat group ($F(2,65) = 30.17$, $P_{(adj)} = 4.9e^{-9}$, 1-ß = 0.97), and no significant effect of task order among groups for this task ($F(4,65) = 1.29$, $P_{(adj)} = 0.36$). Furthermore, there were no significant differences among groups for either locomotor behavior or object exploration during the 15 min habituation session (all $P_{(adj)} > 0.30$). Tukey's HSD post hoc pairwise comparisons demonstrated that the High CGG repeat group performed significantly worse than the Low CGG repeat group and WT group (both $P_{(adj)} < 0.001$), and the Low CGG group performed worse than the WT group ($P_{(adj)} < 0.01$).

To characterize any possible relationship between CGG repeat length and categorical spatial processing in CGG animals with expanded CGG trinucleotide repeats, a correlation coefficient was calculated. A negative association was observed between the CGG trinucleotide repeat length and the ratio

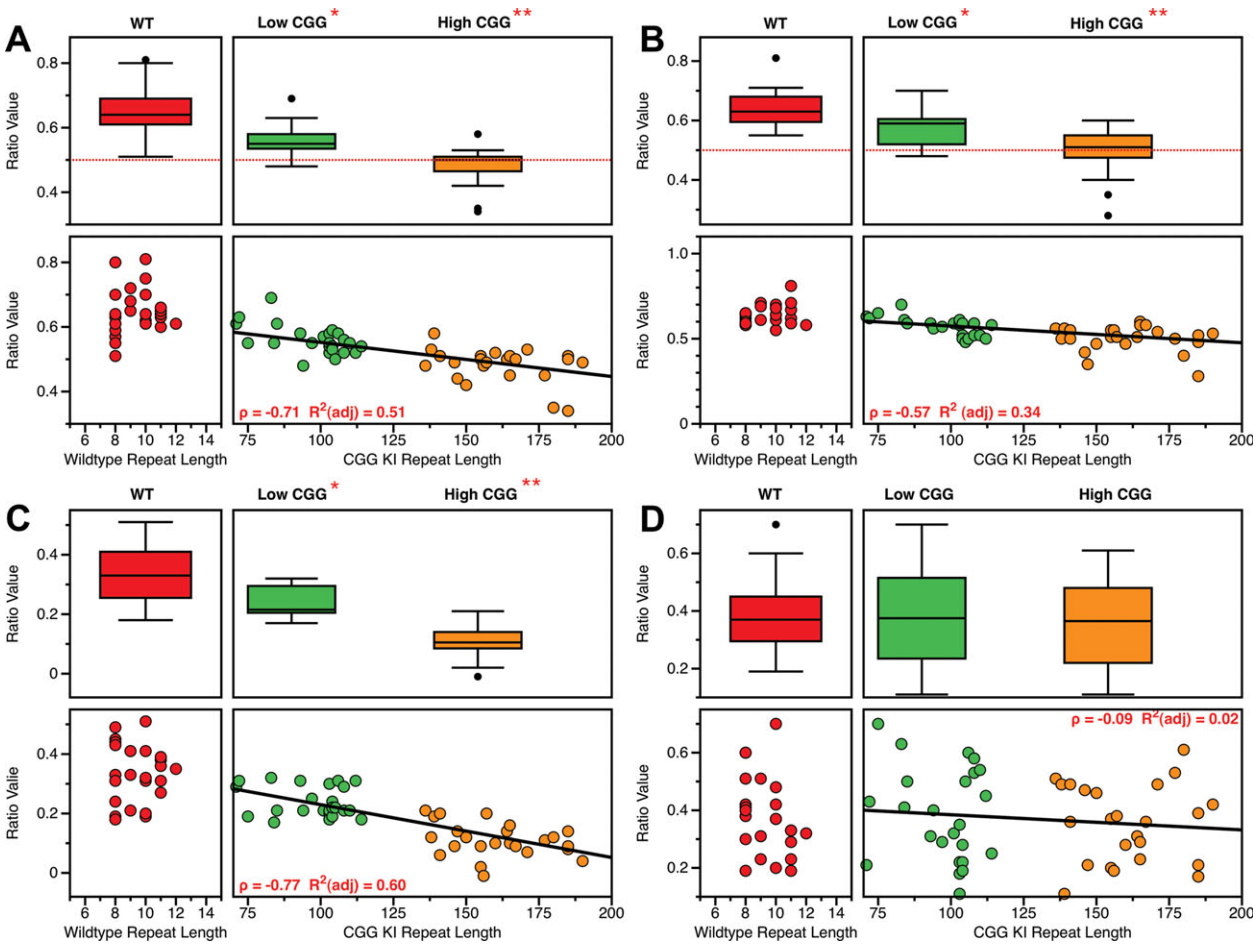

FIGURE 1. CGG repeats modulate behavior in CGG KI Mice. A: Performance during the coordinate spatial information processing task. All CGG KI mice performed more poorly than WT mice for this task, with High CGG repeat mice showing no re-exploration of moved objects. There is a strong negative relationship between CGG repeat length and behavioral performance, suggesting CGG repeat length modulates coordinate spatial processing. B: Performance during the categorical spatial information processing task. All CGG KI mice performed more poorly than WT mice for this task, with High CGG repeat mice showing no re-exploration of transposed objects. There is a strong negative relationship between CGG repeat length and behavioral performance, suggesting CGG repeat length modulates categorical spatial processing. C: Performance during the temporal order for visual objects task. All CGG KI mice performed more poorly than WT mice for this task. There is a strong negative relationship between CGG repeat length and behavioral performance, suggesting CGG repeat length modulates temporal processing. D: Performance during the novelty detection for visual objects task. All mice performed similarly on this task and there is no relationship between CGG repeat length and behavioral performance. *$P < 0.01$, **$P < 0.001$. Red = WT, Green = Low CGG, Orange = High CGG. [Color figure can be viewed in the online issue, which is available at wileyonlinelibrary.com.]

value during performance of the categorical task (Fig. 1B; corr $\rho = -0.57$; $P_{(adj)} = 05.79e^{-12}$, $R^2_{(adj)} = 0.34$).

Temporal Ordering for Visual Objects

For the temporal ordering for visual objects task, there was a significant main effect of CGG repeat group ($F(2,65) = 61.33$, $P_{(adj)} = 1.2e^{-14}$, 1-ß = 0.99), and no effect of task order among groups for this task ($F(4,65) = 1.78$, $P_{(adj)} = 0.70$). Furthermore, there were no significant differences among groups for either locomotor behavior or object exploration during the three, 5 min object presentation sessions (all $P_{(adj)} > 0.25$). Tukey's HSD post hoc pairwise comparisons demonstrated that the High CGG repeat group performed significantly worse than the Low CGG repeat group and WT group (both $P_{(adj)} < 0.001$), and the Low CGG group performed worse than the WT group ($P_{(adj)} < 0.01$).

To characterize any possible relationship between CGG repeat length and temporal ordering for visual object information in CGG animals with expanded CGG trinucleotide repeats, a correlation coefficient was calculated. A negative association was observed between the CGG trinucleotide repeat length and the ratio value during performance of the temporal ordering task (Fig. 1C; corr $\rho = -0.77$; $P_{(adj)} = 3.2e^{-16}$, $R^2_{(adj)} = 0.60$).

Novelty Detection for Visual Objects

For the visual object novelty detection task, there were no significant effect for CGG repeat group ($F(2,65) = 0.24$, $P_{(adj)}$

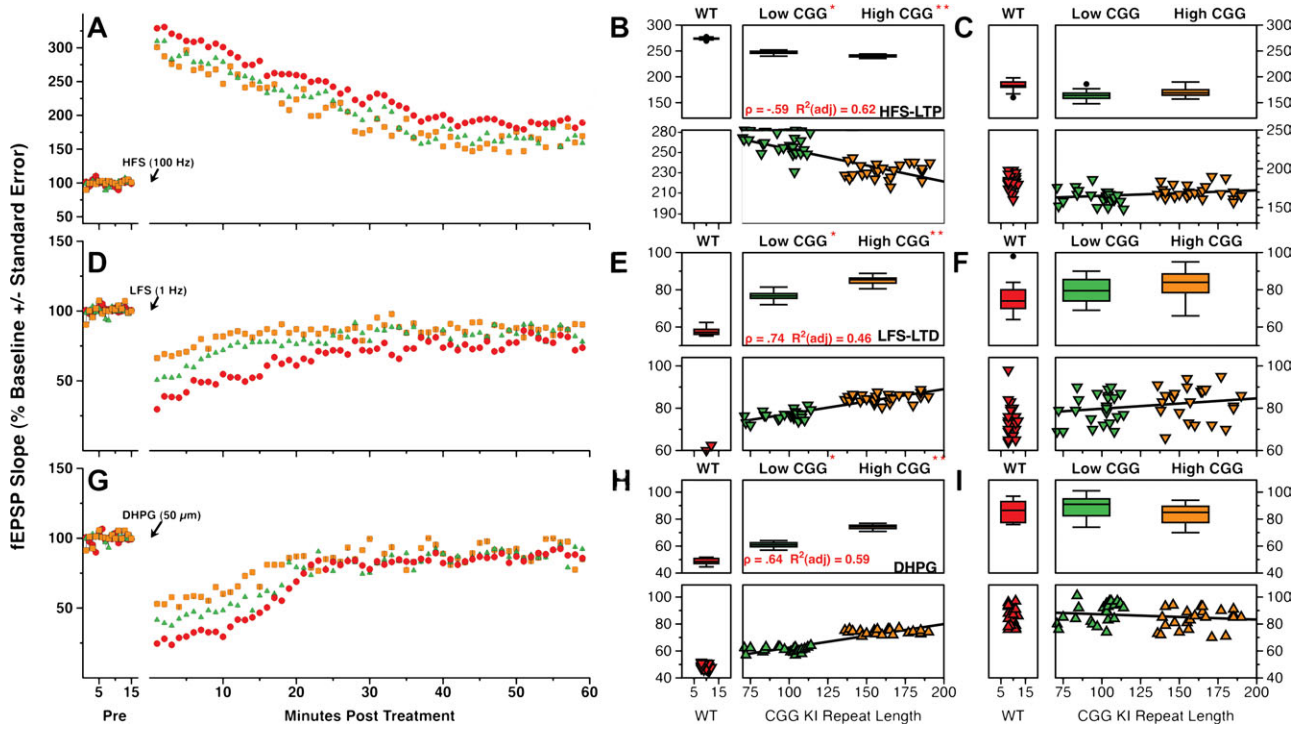

FIGURE 2. CGG repeats modulate neurophysiological responses in CGG KI Mice. A: fEPSP slope (% baseline) pre and post NMDA receptor-dependent LTP induction. All CGG KI mice show reduced LTP induction than WT mice. B: fEPSP slope during min 10–20. There is a strong negative relationship between CGG repeat length and fEPSP slope, suggesting CGG repeat length negatively affects induction of NMDA receptor-dependent LTP. C: fEPSP slope during min 40–50. There is no relationship between CGG repeat length and fEPSP slope, suggesting CGG repeat length does not affect expression of NMDA receptor-dependent LTP once evoked. D: fEPSP slope (% baseline) pre- and post-NMDA receptor-dependent LTD. All CGG KI mice show reduced induction of LTD than WT mice. E: fEPSP slope during min 10–20. There is a strong positive relationship between CGG repeat length and fEPSP slope, suggesting CGG repeat length negatively affects induction of NMDA receptor-dependent LTD. F: fEPSP slope during min 40–50. There is no relationship between CGG repeat length and fEPSP slope, suggesting CGG repeat length does not affect expression of NMDA receptor-dependent LTD once evoked. G: fEPSP slope (% baseline) pre- and post-mGluR1/5 receptor-dependent LTD. All CGG KI mice show less LTD than WT mice. Insets are scaled traces demonstrating these differences. H: fEPSP slope during min 10–20. There is a strong positive relationship between CGG repeat length and fEPSP slope, suggesting CGG repeat length negatively affects induction of mGluR1/5 receptor-dependent LTP. I: fEPSP slope during min 40–50. There is no relationship between CGG repeat length and fEPSP slope, suggesting CGG repeat length does not affect expression of mGluR1/5 receptor-dependent LTD once evoked.*P < 0.01, **P < 0.001. Red = WT, Green = Low CGG, Orange = High CGG. [Color figure can be viewed in the online issue, which is available at wileyonlinelibrary.com.]

= 0.96, 1-ß = 0.99), and no effect of task order among groups for this task (F(4,65)=.16, $P_{(adj)}$ = 0.93). Furthermore, there were no significant differences among groups for either locomotor behavior or object exploration during the three, 5 min object presentation sessions (all $P_{(adj)} > 0.25$).

To verify there was no significant relationship between CGG repeat length and visual object novelty detection information in CGG animals with expanded CGG trinucleotide repeats, a correlation coefficient was calculated. No association was observed between the CGG trinucleotide repeat length and the ratio value during performance of the visual object novelty detection (Fig. 1D; corr ρ = −0.09; $P_{(adj)}$ = 0.5, $R^2_{(adj)}$ = 0.02).

NMDA Receptor-Dependent Long-Term Potentiation

For the NMDA receptor-dependent LTP measures, there was a significant effect of both CGG repeat group (F(2,4243) = 197.14, $P_{(adj)} = 2e^{-16}$, 1-ß = 0.96), and 1 min time bin (F(59,4243) = 172.15, $P_{(adj)} = 2e^{-16}$, 1-ß = 0.97), as well as a significant group × bin interaction (F(59,4243) = 1.09 $P_{(adj)}$ = 0.29, 1-ß = 0.98) (Fig. 2A). Further ANCOVA were performed to characterize these effects.

For the NMDA receptor-dependent LTP, during min 10–20 there was a significant effect for CGG repeat group (F(2,67) = 297.53, $P_{(adj)} = 2.4e^{-15}$, 1-ß = 0.99), and no effect of task order among groups (F(3,67) = 0.01, $P_{(adj)}$ = 0.96), mouse age (F(3,67) = 0.13, $P_{(adj)}$ = 0.85), nor order in which each hippocampal slice was used (F(2,67)=.06, $P_{(adj)}$ = 0.91). Tukey's HSD post hoc pairwise comparisons demonstrated that the High CGG repeat group has significantly less LTP than the Low CGG repeat group and WT group (both $P_{(adj)} < 0.001$), and the Low CGG group had less LTP than the WT group ($P_{(adj)} < 0.01$). However, during 40–50 min post conditioning there were no differences among the groups (all $P_{(adj)} > 0.15$).

To characterize the relationship between CGG repeat length and NDMA receptor-dependent LTP in CGG animals with expanded CGG trinucleotide repeats, a correlation coefficient was calculated. A negative association was observed between the CGG trinucleotide repeat length and fEPSP slope during min 10–20, suggesting increasingly poor LTP as a function of CGG repeat length (Fig. 2B; corr $\rho = -0.59$; $P_{(adj)} < 2.2e^{-16}$, $R^2_{(adj)} = 0.62$). No association was observed between the CGG trinucleotide repeat lengths and fEPSP slope during min 40–50, suggesting no effect of CGG repeat length on this later phase of plasticity (Fig. 2C; corr $\rho = -0.1$; $P_{(adj)} = 0.24$, $R^2_{(adj)} = 0.09$).

NMDA Receptor-Dependent Long-Term Depression

For the NMDA receptor-dependent LTD, there was a significant effect of both CGG repeat group ($F(2,4243)=210.04$, $P_{(adj)} = 2e^{-16}$, 1-ß = .98), and 1 min time bin ($F(59,4243) = 104.82$, $P_{(adj)} = 2e^{-16}$, 1-ß = 0.99), as well as a significant group × bin interaction ($F(59,4243) = 150.01$ $P_{(adj)} = 5.7e^{-9}$, 1-ß = 0.98) (Fig. 2D). Further ANCOVA were performed to characterize these effects.

For the NMDA receptor-dependent LTD, during min 10–20 there was a significant effect for CGG repeat group ($F(2,67) = 184.59$, $P_{(adj)} = 2.4e^{-15}$, 1-ß = 0.97), and no effect of task order among groups ($F(3,67) = 1.72$, $P_{(adj)} = 0.86$), mouse age ($F(3,67)=.08$, $P_{(adj)} = 0.94$), nor order in which each hippocampal slice was used ($F(2,67) = 1.10$, $P_{(adj)} = 0.83$). Tukey's HSD post hoc pairwise comparisons demonstrated that the High CGG repeat group has significantly greater LTD than the Low CGG repeat group and WT group (both $P_{(adj)} < 0.001$), and the Low CGG group had greater LTD than the WT group ($P_{(adj)} < 0.01$). However, during min 40–50 there were no main effects (all $P_{(adj)} > 0.45$).

To characterize the relationship between CGG repeat length and NMDA receptor-dependent LTD in CGG animals with expanded CGG trinucleotide repeats, a correlation coefficient was calculated. A positive association was observed between the CGG trinucleotide repeat length and fEPSP slope during min 10–20, indicating increasing LTD as a function of CGG repeat length (Fig. 2E; corr $\rho = 0.74$; $P_{(adj)} < 2.2e^{-16}$, $R^2_{(adj)} = 0.46$). No association was observed between the CGG trinucleotide repeat lengths and fEPSP slope during min 40–50, suggesting no effect of CGG repeat length on this later phase of plasticity (Fig. 2F; corr $\rho = 0.02$; $P_{(adj)} = 0.45$, $R^2_{(adj)} = 0.01$).

mGluR1/5 Receptor-Dependent Long-Term Depression

For the mGluR1/5 receptor-dependent LTD measures, there was a significant effect of both CGG repeat group ($F(2,4243) = 195.4$, $P_{(adj)}=2e^{-16}$, 1-ß = 0.98), and 1 min time bin ($F(59,4243) = 301.57$, $P_{(adj)} = 2e^{-16}$, 1-ß = 0.99), as well as a significant group x bin interaction ($F(59,4243) = 160.88$, $P_{(adj)} = 5.9e^{-9}$, 1-ß = 0.95) (Fig. 2G). Further ANCOVA were performed to characterize these effects.

For the mGluR1/5 receptor-dependent LTD, during min 10–20 there was a significant effect for CGG repeat group ($F(2,67)=203.21$, $P_{(adj)} = 2.4e^{-15}$, 1-ß = 0.97), and no effect of task order among groups ($F(3,67)=.47$, $P_{(adj)} = 0.98$), mouse age ($F(3,67)=.55$, $P_{(adj)} = 0.91$), nor order in which each hippocampal slice was used ($F(2,67)=1.85$, $P_{(adj)} = 0.79$). Tukey's HSD post hoc pairwise comparisons demonstrated that the High CGG repeat group has significantly greater LTD than the Low CGG repeat group and WT groups (both $P_{(adj)} < 0.001$), and the Low CGG group had greater LTD than the WT group ($P_{(adj)} < 0.01$). However, during min 40–50 there were no main effects (all $P_{(adj)} > 0.54$).

To characterize the relationship between CGG repeat length and mGluR1/5 receptor-dependent LTD in CGG animals with expanded CGG trinucleotide repeats, a correlation coefficient was calculated. A positive association was observed between the CGG trinucleotide repeat length and fEPSP slope during min 10–20, indicating increasing mGluR1/5 receptor-dependent LTD as a function of CGG repeat length (Fig. 2H; corr $\rho = 0.64$; $P_{(adj)} < 2.2e^{-16}$, $R^2_{(adj)} = 0.59$). No association was observed between the CGG trinucleotide repeat lengths and fEPSP slope during min 40–50, suggesting no effect of CGG repeat length on this later phase of plasticity (Fig. 2I; corr $\rho = 0.05$; $P_{(adj)} = 0.39$, $R^2_{(adj)} = 0.03$).

Classification of Mice by CGG Repeat Length Using Cluster Analysis

Unsupervised hierarchal cluster analysis was first performed to investigate whether CGG KI mice separated according to CGG repeat length. The dendrograms based on the performance on behavioral and neurophysiological experiments showed clear separation between WT and CGG KI mice into two distinct clusters (Figs. 3A,B). Furthermore, within the CGG KI mouse cluster the Low CGG KI mice, defined as mice with 70–116 CGG repeats were perfectly separated into a unique cluster from the High CGG mice defined as mice having 132–198 CGG repeats. Furthermore, CGG KI mice were correctly grouped into similar CGG repeat length sub-clusters in the Low CGG repeat group and nearly correctly in the High CGG repeat group.

Identifying the Groups of Like Experiments Using Cluster Analysis

Similarly unsupervised hierarchal cluster analysis was performed to identify patterns and clusters among the different experiments and express the data in such a way to highlight similarities and differences. The novelty detection task, appeared to have no correlation with the CGG repeat length, and was separated from the other behavioral tasks. From there, the coordinate spatial processing and temporal ordering for visual objects task placed in the same cluster and together segregated animals well according to the CGG repeat length grouping. The categorical spatial processing task was less correlated

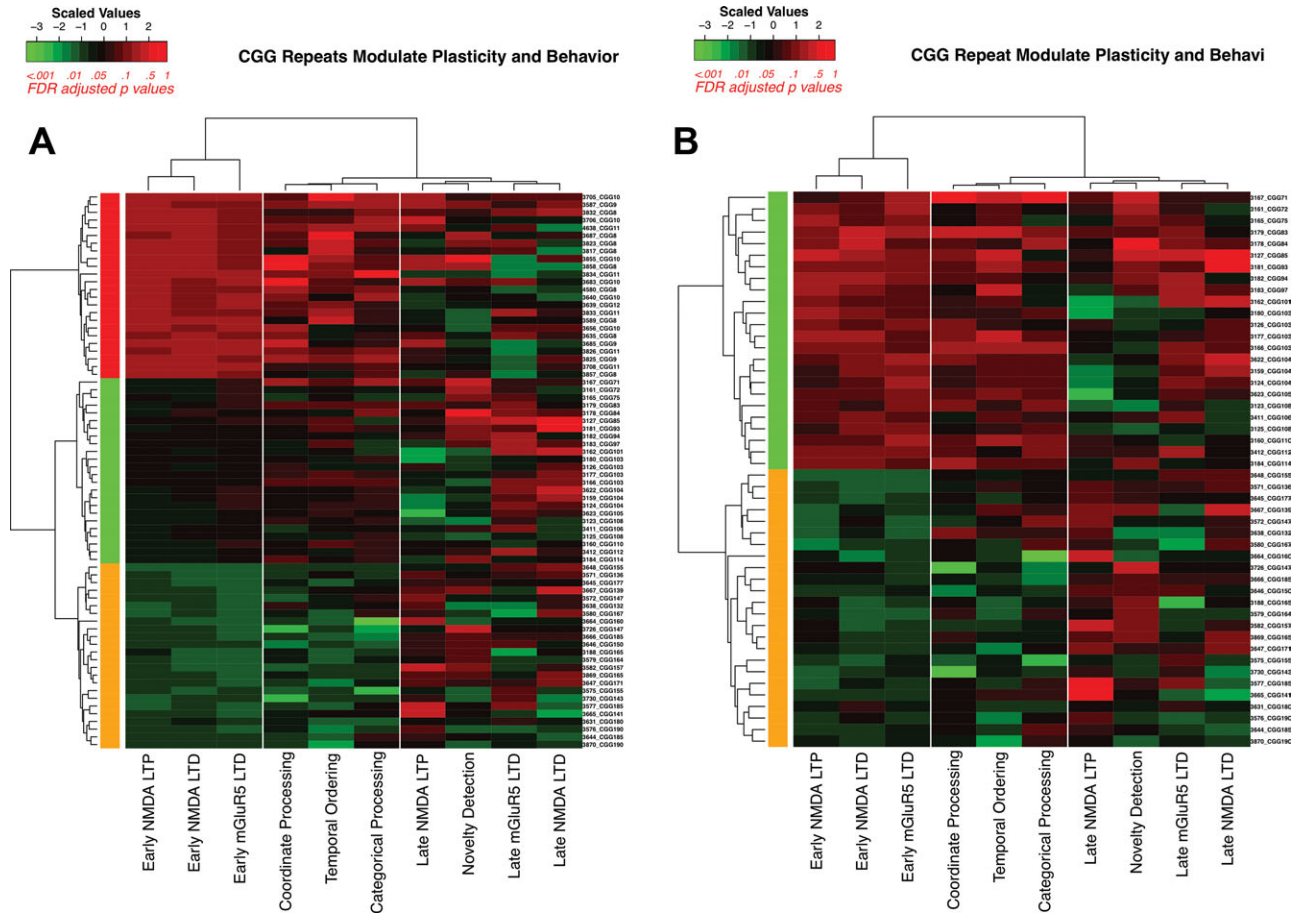

FIGURE 3. CGG repeat length directly modulates physiology and spatiotemporal performance. A: Predictive validity of classifier. Behavioral performance and physiological measures discriminate WT mice from CGG KI mice, and further discriminate CGG KI mice with 70–116 CGG repeats from CGG KI mice with 132–200 CGG repeats. The colored bars along the left correspond to animal group as arbitrarily defined by the unsupervised clustering algorithm and match the colors used for the plotted data in Figure 1. The dendrogram along the top demonstrates the relationships among experiments performed with these CGG KI mice. White bars were places on the heatmap separating columns that belong to different clusters. B: Predictive validity of classifier within CGG KI mice. Early LTP/LTD refers to min 10–20 post induction. Late LTP/LTD refers to min 40–50 post induction. Bars along the right side of the heatmap correspond to group identity: Red = WT, Green = Low CGG, Orange = High CGG. [Color figure can be viewed in the online issue, which is available at wileyonlinelibrary.com.]

with not only the coordinate and temporal tasks, but also CGG repeat length. When WT mice were excluded from the analysis and only CGG KI mice were included, the same groupings emerged within the CGG KI mice as well as the task groupings. This observation suggests that there was distinct separation of the Low CGG repeat group cluster from the High CGG repeat cluster.

For the physiological data, NMDA receptor-dependent LTP and LTD induction at min 10–20 were grouped into the same cluster, and showed similarities between them. mGluR1/5 dependent LTD induction at min 10–20 was more related to NMDA receptor-dependent plasticity and the CGG repeat category than behavior, but their similarities to NMDA receptor-dependent LTP and LTD induction was less profound. As mentioned above, all plasticity measures at 40–50 min post induction were nonpredictive and were placed in the same cluster as the novelty detection behavioral task. These findings were consistent when only the CGG KI mice were analyzed. Importantly, all measures of plasticity at min 10–20 were in a single larger cluster that was independent of all behavioral tasks and plasticity at min 40–50, which were placed in separate clusters by the analysis.

Prediction of Sample Classification of CGG KI Mice by Repeat Length

The cluster analysis results showed differences between the CGG repeat groups and similarities of phenotypic profiles within a CGG repeat group (Fig. 3B). Thus we investigated whether phenotypic values of experiments could make inference about CGG repeat length of CGG KI mice. SVM (Support Vector Machines) was carried out to derive a linear classifier comprised of task performance scores that can classify the CGG KI mice by repeat length (i.e., Low CGG repeat vs.

High CGG repeat) using a training set. The predictive performance of the linear classifier was validated using test samples.

When the classifier was developed based on scores for the coordinate spatial processing and temporal ordering, the classifier performed well with 92% accuracy based on iterative 5-fold CV (94% based on 10-fold CV; Fig. 4B). When the categorical spatial task was added to the model, a poor classification was attained as expected due to the lack of separation between the coordinate spatial processing and temporal ordering task and categorical spatial task as shown in clustering, only classifying 69% of the CGG KI mice correctly based on iterative 5-fold CV (71% based on 10-fold CV; Fig. 4A). With inclusion of the WT mice, the model improved the classification of the CGG KI mice using the coordinate and temporal order experiments to 98% accuracy, but adding the categorical task into the model still reduced the predictive power of the model to 75% accuracy based on 5-fold CV (78% based on 10-fold CV). Addition of the novelty detection task resulted in a large decrease in predictive value of the model, resulting in correct classification of only 44% of the mice based on 5-fold CV (48% based on 10-fold CV; data not shown).

In the case where the coordinate and temporal order tasks were used to correctly classify the CGG KI mice by repeat group 92% of the time, the four misclassified mice into the Low CGG repeat group were the four mice with the lowest number of CGG repeats (132, 136, 138, and 141 CGG repeats) in the High CGG repeat group. In no cases were mice from the Low CGG repeat group misclassified as High CGG repeat mice. In cases where 5-fold and 10-fold CV provide different results for the classification, the mouse with 141 repeats was correctly classified into the High CGG repeat group by iterative 10-fold CV, while 5-fold CV misclassified this mouse into the Low CGG repeat group. Iterative three-fold CV and leave one out CV all gave the same classifications as 5-fold CV for all classifications.

When the classifier was developed based on scores for the NMDA receptor-dependent LTP and LTD induction measures at min 10–20 and 40–50, the classifier performed with 100% accuracy based on iterative 5-fold CV (100% based on 10-fold CV; Fig. 4C). When the mGluR1/5 dependent LTD was added to the model, the classifications did not change, still classifying mice into CGG repeat groups with 100% accuracy based on iterative 5-fold CV (100% based on 10-fold CV; Fig. 4D).

DISCUSSION

Previous analyses of CGG KI mouse cognitive function have been unable to conclusively determine any direct relationships between CGG repeat length and cognitive function due to insufficient sample size and incomplete coverage of the premutation range (i.e., 70–200 repeats; Hunsaker et al., 2009, 2010, 2011b; Diep et al., 2012). The behavioral results previously reported in the CGG KI and CGG-CCG mice, unfortunately, did not directly model the reports in carriers of the premutation (van Dam et al., 2005; Qin et al., 2011).

In fact, only few reports in the human premutation have been able to demonstrate similar relationships between genetic dosage and neurocognitive function, but were limited by a confined CGG repeat ranges and a wide range of ages in their studies (CGG range 67–143 repeats, age range 21–42 years of age; Goodrich-Hunsaker et al., 2011a,b,c). The present report overcomes this challenge and provides clear evidence for a linear inverse relationship between cognitive function and CGG repeat length in CGG KI mice at a single time point (9 months of age). Specifically, the CGG KI mice showed CGG repeat length modulated deficits for spatial and temporal processing, but spared novel object detection (Fig. 1). These data argue for specific impairments in spatiotemporal processing with intact sensory/perceptual function, suggesting impaired spatial and temporal pattern separation underlie some cognitive dysfunction in the premutation (cf., Johnson-Glenberg, 2008; Simon, 2011).

Furthermore, the CGG KI mice had CGG repeat length modulated reductions in NMDA receptor-dependent LTP and LTD induction, as well as mGluR1/5 dependent LTD induction at the Schaffer collateral synapse (i.e., by generally reducing induction, but not expression, of neuronal plasticity in the hippocampus; Fig. 2). Importantly, as induction, but not expression, of both NMDA and mGluR1/5 dependent plasticity appear to be similarly disrupted by increasing CGG repeat lengths, it appears likely that the observed reductions in plasticity induction resulted from a general disruption of neuronal function, as opposed to effects selectively acting upon one receptor system over another, as has been described in FXS (*e.g.,* mGluR1/5 LTD enhancement; Bear et al., 2004). Furthermore, it has recently been demonstrated that the CGG KI mouse shown a small but significant reduction in dendritic complexity as well as spine density in pyramidal neurons of visual cortex (Berman et al., 2012), and a similar trend appears in CA1 pyramidal neurons (unpublished observations). These dendritic abnormalities may underlie the reduced plasticity observed in CGG KI mice relative to wildtype littermate animals. These data support models that propose elevations in *Fmr1* mRNA underlie premutation neuropathology as *Fmr1* mRNA expression scales linearly with CGG repeat length across the premutation range, whereas Fmrp levels show significant reductions only as the CGG repeat lengths approach 200 (Jin et al., 2003; Brouwer et al., 2008; Tassone et al., 2008; Raske and Hagerman, 2009; Hoem et al., 2011). Alternate possibilities are that the effects of mitochondrial dysfunction in the premutation (Ross-Inta et al., 2010; Napoli et al., 2011) or some unknown metabolic or physiological abnormality in neurons reduces neuronal viability in vitro (Chen et al., 2010).

To better characterize the utility of the behavioral tasks and measures of plasticity to separate CGG KI mice into groups corresponding to CGG repeat length, a hierarchal cluster analysis was performed using only the physiological and behavioral data and shown in Figure 3. The CGG KI mice were separated

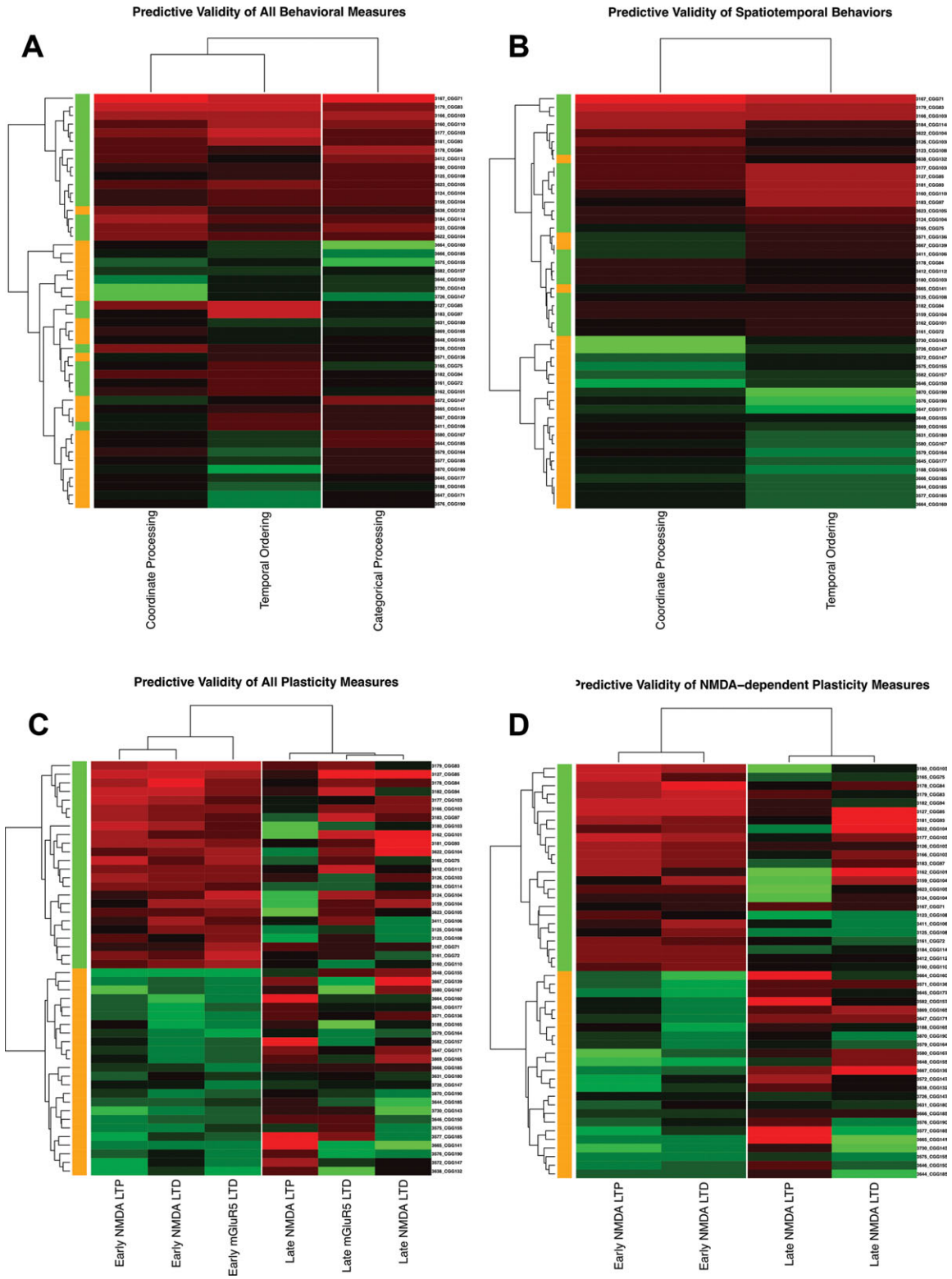

FIGURE 4. Physiology and spatiotemporal behavioral performance can be used to predict CGG repeat length. A: Behavioral measures including the temporal ordering, coordinate and categorical processing task was only able to classify the CGG repeat groups with 69% accuracy, however (B) the cluster containing coordinate spatial processing and temporal ordering tasks alone, excluding the categorical task, improved the performance of the classifier to 92% accuracy. C: All plasticity measures were able to correctly classify mice by CGG repeat length, and (D) even just the NMDA receptor-dependent physiological measures were sufficient to correctly classify CGG KI mice. All classification based on 5-fold cross validation. Early LTP/LTD refers to min 10–20 post induction. Late LTP/LTD refers to min 40–50 post induction. Bars along the right side of the heatmap correspond to group identity: Green = Low CGG, Orange = High CGG. [Color figure can be viewed in the online issue, which is available at wileyonlinelibrary.com.]

into two groups corresponding to mice with 70–116 CGG repeats in one group (Low CGG; green in all figures) and mice with 132–198 CGG repeats in the second group (High CGG; orange in all figures). Again it must be mentioned that these CGG repeat groupings emerged in the mouse colony through breeding, and do not reflect different states among human fragile × premutation carriers so far as has been reported. Furthermore, when all experiments were included in the clustering, the CGG KI mice were correctly grouped according to CGG repeat length within the Low CGG repeat group, but less so in the High CGG repeat group.

The classification analysis suggest that a mouse's performance on these spatiotemporal processing tasks and measures of plasticity are sufficient to classify CGG KI mice by CGG repeat length within the premutation length to 92% accuracy based on 5-fold cross validation (CV; Fig. 3B). In other words, these experiments serve as a behavioral endophenotype that can be used to determine the severity of the PM, at least in the CGG KI mouse model. Intriguingly, the two behavioral tasks demonstrating the highest predictive validity (coordinate and temporal ordering tasks) were also the tasks demonstrated previously to require fine-scale spatial or temporal attention/pattern separation processes shown to require hippocampal integrity (Kesner et al., 2004; Goodrich-Hunsaker et al., 2005; Rolls and Kesner, 2006; Kesner and Goodrich-Hunsaker, 2010). The categorical task has been shown to depend primarily upon the neocortex and utilizes a more coarse level of spatial processing (Goodrich-Hunsaker et al., 2005; Hunsaker et al., 2009), and the novelty detection task (which proved nonpredictive) depends upon a distributed network involving rostral and rhinal cortices (Cowell et al., 2010; McTighe et al., 2010).

Together these findings suggest the feasibility of developing a behavioral endophenotype that can be used to predict cognitive dysfunction in CGG KI mice. More to the point, it appears that a focus on tasks evaluating spatial and temporal pattern separation can be used to classify the CGG KI mice by repeat lengths with 92% certainty. Inclusion of performance measures from tasks that do not emphasize spatial or temporal attention/pattern separation (i.e., categorical spatial processing and novelty detection) do not contribute to the classification. This hypothesis is supported by the classification analyses, which demonstrate clearly that spatiotemporal processing and measures of synaptic plasticity are sufficient to predict dosage of the premutation in he CGG KI mice. Evidence for a direct effect of the dosage or size of the premutation on behavioral and neurophysiological measures is the definition of an endophenotype (Gottesman and Gould, 2003; Hunsaker, 2012).

It is important to state the categorical task was useful to clearly separate CGG KI mice from WT mice, but proved to be unsuitable to classify CGG KI mice by CGG repeat lengths. What these data suggest is that the coordinate spatial processing and temporal ordering tasks were not only predictive to classify WT mice from CGG KI mice, but critically, the performance on these tasks was directly modulated by the length of the CGG trinucleotide repeat. These data support the spatiotemporal hypergranularity model (Simon, 2008, 2011; Hunsaker, 2012), that posits specific impairments to spatial and temporal attention. As such, an emphasis on behavioral tasks evaluating fine-scale spatial and temporal attention (or pattern separation; Aimone et al., 2011; Hunsaker, 2012; Yassa and Stark, 2012), may be perfectly suited to quantifying the fundamental cognitive disruptions observed in the CGG KI mouse model of the premutation. Although beyond the scope of the present study, the addition of tasks involving a high demand for attention or executive function may improve the behavioral endophenotype reported here (Johnson-Glenberg, 2008; Simon, 2011). Furthermore, these results serve only to provide preliminary support for a behavioral endophenotype in the CGG KI mouse model of the fragile × premutation. Besides executive function, affect, response, social behaviors, and anxiety domains remain untested in the CGG KI mice. Such data would provide more information toward a pattern of not only weaknesses, but also neurocognitive strengths that are modulated by CGG repeat lengths. Furthermore, the present study was unable to elucidate the mechanisms underlying the impaired induction of synaptic plasticity with concomitantly spared expression of evoked plasticity. Further research is necessary to provide answer these questions and uncover the mechanisms by which increasing CGG repeats affect plasticity and cognitive function.

The present experiment provides the first clear demonstration of a CGG repeat length-dependent decline in cognitive function in the premutation across virtually the full extent of premutation CGG repeat lengths. Measures of synaptic plasticity and behavioral tasks requiring spatial and temporal attention were sufficient to classify CGG KI mice by CGG repeat length, even correctly predicting actual CGG repeat length. These data provide a physiological and behavioral biomarker in CGG KI mice that may be used as an outcome measure for studies into treatment options for the premutation or else to predict disease severity or eventual progression toward a neurodegenerative trajectory.

Acknowledgments

The authors thank Drs. Philip A. Schwartzkroin and Naranzogt Tschuluun, Ph.D. as well as Erik W. Schluter for assistance with neurophysiological experiments; Drs. Yi Michelle Deng, Ph.D. and Naomi J. Goodrich-Hunsaker, Ph.D. for helpful conversations concerning the application of hierarchal clustering techniques for behavioral performance, and Drs. Raymond P. Kesner and Philip A. Schwartzkroin for a critical reading of the manuscript.

REFERENCES

Aimone JB, Deng W, Gage FH. 2011. Resolving new memories: A critical look at the dentate gyrus, adult neurogenesis, and pattern separation. Neuron 70:589–596.

Bear MF, Huber KM, Warren ST. 2004. The mGluR theory of fragile × mental retardation. Trends Neurosci 27:370–377.

Benjamini Y, Drai D, Elmer G, Kafkafi N, Golani I. 2001. Controlling the false discovery rate in behavior genetics research. Behav Brain Res 125(1–2):279–284.

Berman RF, Murray KD, Arque G, Hunsaker MR, Wenzel HJ. 2012. Abnormal dendrite and spine morphology in primary visual cortex in the CGG knock-in mouse model of the fragile X premutation. Epilepsia 53(Suppl 1):149–159.

Brouwer JR, Huizer K, Severijnen LA, Hukema RK, Berman RF, Oostra BA, Willemsen R. 2008. CGG-repeat length and neuropathological and molecular correlates in a mouse model for fragile X-associated tremor/ataxia syndrome. J Neurochem 107:1671–1682.

Chen Y, Tassone F, Berman RF, Hagerman PJ, Hagerman RJ, Willemsen R, Pessah IN. 2010. Murine hippocampal neurons expressing *Fmr1* gene premutations show early developmental deficits and late degeneration. Hum Mol Genet 19:196–208.

Cornish KM, Kogan CS, Li L, Turk J, Jacquemont S, Hagerman RJ. 2009. Lifespan changes in working memory in fragile X premutation males. Brain Cogn 69(3):551–558.

Cowell RA, Bussey TJ, Saksida LM. 2010. Components of recognition memory: Dissociable cognitive processes or just differences in representational complexity? Hippocampus 20:1245–1262.

Diep AA, Hunsaker MR, Kwock R, Kim K, Willemsen R, Berman RF. 2012. Female CGG knock-in mice modeling the fragile X premutation are impaired on a skilled forelimb reaching task. Neurobiol Learn Mem 97:229–234.

Entezam A, Biacsi R, Orrison B, Saha T, Hoffman GE, Grabczyk E, Nussbaum RL, Usdin K. 2007. Regional FMRP deficits and large repeat expansions into the full mutation range in a new Fragile X premutation mouse model. Gene 395(1–2):125–134.

Faul F, Erdfelder E, Buchner A, Lang AG. 2009. Statistical power analyses using G*Power 3.1: tests for correlation and regression analyses. Behav Res Methods 41:1149–1160.

Faul F, Erdfelder E, Lang AG, Buchner A. 2007. G*Power 3: A flexible statistical power analysis program for the social, behavioral, and biomedical sciences. Behav Res Methods 39:175–191.

Goodrich-Hunsaker NJ, Hunsaker MR, Kesner RP. 2005. Dissociating the role of the parietal cortex and dorsal hippocampus for spatial information processing. Behav Neurosci 119:1307–1315.

Goodrich-Hunsaker NJ, Wong LM, McLennan Y, Srivastava S, Tassone F, Harvey D, Rivera SM, Simon TJ. 2011a. Young adult female fragile X premutation carriers show age- and genetically-modulated cognitive impairments. Brain Cogn 75:255–260.

Goodrich-Hunsaker NJ, Wong LM, McLennan Y, Tassone F, Harvey D, Rivera SM, Simon TJ. 2011b. Enhanced manual and oral motor reaction time in young adult female fragile X premutation carriers. J Int Neuropsychol Soc 17:746–750.

Goodrich-Hunsaker NJ, Wong LM, McLennan Y, Tassone F, Harvey D, Rivera SM, Simon TJ. 2011c. Adult female fragile X premutation carriers exhibit age- and CGG repeat length-related impairments on an attentionally based enumeration task. Front Hum Neurosci 5:63.

Gottesman II, Gould TD. 2003. The endophenotype concept in psychiatry: Etymology and strategic intentions. Am J Psychiatry 160: 636–645.

Hanson JE, Madison DV. 2011. Imbalanced pattern completion vs. separation in cognitive disease: Network simulations of synaptic pathologies predict a personalized therapeutics strategy. BMC Neurosci 11:96.

Hessl D, Wang JM, Schneider A, Koldewyn K, Le L, Iwahashi C, Cheung K, Tassone F, Hagerman PJ, Rivera SM. 2011. Decreased fragile X mental retardation protein expression underlies amygdala dysfunction in carriers of the fragile X premutation. Biol Psychiatry 70:859–865.

Hoem G, Raske CR, Garcia-Arocena D, Tassone F, Sanchez E, Ludwig AL, Iwahashi CK, Kumar M, Yang JE, Hagerman PJ. 2011. CGG-repeat length threshold for *FMR1* RNA pathogenesis in a cellular model for FXTAS. Hum Mol Genet 20:2161–2170.

Hunsaker MR. 2012. Comprehensive neurocognitive endophenotyping strategies for mouse models of genetic disorders. Prog Neurobiol 96:220–241.

Hunsaker MR, Greco CM, Tassone F, Berman RF, Willemsen R, Hagerman RJ, Hagerman PJ. 2011a. Rare intranuclear inclusions in the brains of 3 older adult males with fragile x syndrome: implications for the spectrum of fragile x-associated disorders. J Neuropathol Exp Neurol 70:462–469.

Hunsaker MR, Goodrich-Hunsaker NJ, Willemsen R, Berman RF. 2010. Temporal ordering deficits in female CGG KI mice heterozygous for the fragile X premutation. Behav Brain Res 213:263–268.

Hunsaker MR, von Leden RE, Ta BT, Goodrich-Hunsaker NJ, Arque G, Kim K, Willemsen R, Berman RF. 2011b. Motor deficits on a ladder rung task in male and female adolescent and adult CGG knock-in mice. Behav Brain Res 222:117–121.

Hunsaker MR, Wenzel HJ, Willemsen R, Berman RF. 2009. Progressive spatial processing deficits in a mouse model of the fragile X premutation. Behav Neurosci 123:1315–1324.

Hunter JE, Rohr JK, Sherman SL. 2010. Co-occurring diagnoses among *FMR1* premutation allele carriers. Clin Genet 77:374–381.

Hunter JE, Abramowitz A, Rusin M, Sherman SL. 2009. Is there evidence for neuropsychological and neurobehavioral phenotypes among adults without FXTAS who carry the *FMR1* premutation? A review of current literature. Genet Med 11:79–89.

Jin P, Zarnescu DC, Zhang F, Pearson CE, Lucchesi JC, Moses K, Warren ST. 2003. RNA-mediated neurodegeneration caused by the fragile X premutation rCGG repeats in Drosophila. Neuron 39:739–747.

Johnson-Glenberg MC. 2008. Fragile X syndrome: Neural network models of sequencing and memory. Cogn Syst Res 9:274–292.

Kéri S, Benedek G. 2010. The perception of biological and mechanical motion in female fragile X premutation carriers. Brain Cogn 72:197–201.

Kéri S, Benedek G. 2009. Visual pathway deficit in female fragile X premutation carriers: A potential endophenotype. Brain Cogn 69:291–295.

Kesner RP. 2007. A behavioral analysis of dentate gyrus function. Prog Brain Res 163:567–576.

Kesner RP, Goodrich-Hunsaker NJ. 2010. Developing an animal model of human amnesia: The role of the hippocampus. Neuropsychologia 48:2290–2302.

Kesner RP, Lee I, Gilbert P. 2004. A behavioral assessment of hippocampal function based on a subregional analysis. Rev Neurosci 15:333–351.

Koldewyn K, Hessl D, Adams J, Tassone F, Hagerman PJ, Hagerman RJ, Rivera SM. 2008. Reduced hippocampal activation during recall is associated with elevated *FMR1* mRNA and psychiatric symptoms in men with the fragile X Premutation. Brain Imaging Behav 2:105–116.

McTighe SM, Cowell RA, Winters BD, Bussey TJ, Saksida LM. 2010. Paradoxical false memory for objects after brain damage. Science 330:1408–1410.

Napoli E, Ross-Inta C, Wong S, Omanska-Klusek A, Barrow C, Iwahashi C, Garcia-Arocena D, Sakaguchi D, Berry-Kravis E, Hagerman R, Hagerman PJ, Giulivi C. 2011. Altered zinc transport disrupts mitochondrial protein processing/import in fragile X-associated tremor/ataxia syndrome. Hum Mol Genet 20:3079–3092.

Qin M, Entezam A, Usdin K, Huang T, Liu ZH, Hoffman GE, Smith CB. 2011. A mouse model of the fragile X premutation: Effects on behavior, dendrite morphology, and regional rates of cerebral protein synthesis. Neurobiol Dis 42:85–98.

R Development Core Team. 2011. R: A language and environment for statistical computing. R Foundation for Statistical Computing, Vienna, Austria. ISBN3-900051-07-0, URL Available at: http://www.R-project.org/.

Raske C, Hagerman PJ. 2009. Molecular pathogenesis of fragile X-associated tremor/ataxia syndrome. J Investig Med 57:825–829.

Rolls ET, Kesner RP. 2006. A computational theory of hippocampal function, and empirical tests of the theory. Prog Neurobiol 79:1–48.

Ross-Inta C, Omanska-Klusek A, Wong S, Barrow C, Garcia-Arocena D, Iwahashi C, Berry-Kravis E, Hagerman RJ, Hagerman PJ, Giulivi C. 2010. Evidence of mitochondrial dysfunction in fragile X-associated tremor/ataxia syndrome. Biochem J 429:545–552.

Saluto A, Brussino A, Tassone F, Arduino C, Cagnoli C, Pappi P, Hagerman P, Migone N, Brusco A. 2005. An enhanced polymerase chain reaction assay to detect pre- and full mutation alleles of the fragile X mental retardation 1 gene. J Mol Diagnosis 7:605–612.

Simon TJ. 2008. A new account of the neurocognitive foundations of impairments in space, time and number processing in children with chromosome 22q11.2 deletion syndrome. Dev Disabil Res Rev 14:52–58.

Simon TJ. 2011. Clues to the foundations of numerical cognitive impairments: Evidence from genetic disorders. Dev Neuropsychol 36:788–805.

Tassone F, Hagerman RJ, Taylor AK, Gane LW, Godfrey TE, Hagerman PJ. 2000. Elevated levels of *FMR1* mRNA in carrier males: a new mechanism of involvement in the fragile-X syndrome. Am J Hum Genet 66:6–15.

Tassone F, Hagerman RJ, Taylor AK, Mills JB, Harris SW, Gane LW, Hagerman PJ. 2000. Clinical involvement and protein expression in individuals with the *FMR1* premutation. Am J Med Genet 91:144–152.

Tassone F, Pan R, Amiri K, Taylor AK, Hagerman PJ. 2008. A rapid polymerase chain reaction-based screening method for identification of all expanded alleles of the fragile X (*FMR1*) gene in newborn and high-risk populations. J Mol Diagn 10:43–49.

van Dam D, Errijgers V, Kooy RF, Willemsen R, Mientjes E, Oostra BA, De Deyn PP. 2005. Cognitive decline, neuromotor and behavioural disturbances in a mouse model for fragile-X-associated tremor/ataxia syndrome (FXTAS). Behav Brain Res 162:233–239.

Ward JH Jr. 1963. Hierarchical grouping to optimize an objective function. J Am Stat Assoc 58:236–244.

Yassa MA, Stark CE. 2011. Pattern separation in the hippocampus. Trends Neurosci 34:515–525.